Journal of Solid State Chemistry **163,** 77–83 (2002)
doi:10.1006/jssc.2001.9371, available online at http://www.idealibrary.com on IDEAL®

High-Pressure Synthesis and Crystal Structures of β-*M*N*X* (*M* = Zr, Hf; *X* = Br, I)

Xuean Chen,* Hiroshi Fukuoka,† and Shoji Yamanaka*,†,[1]

*CREST, Japan Science and Technology Corporation (JST), Kawaguchi 332-0012, Japan; and †Department of Applied Chemistry, Graduate School of Engineering, Hiroshima University, Higashi-Hiroshima 739-8527, Japan

Received May 29, 2001; in revised form August 13, 2001; accepted August 22, 2001

The single crystals of four kinds of metal nitride halides, β-*M*N*X* (*M* = Zr, Hf; *X* = Br, I), were prepared in Pt (or Au) capsules by the reaction of *M*N or α-*M*N*X* powders with NH_4X as fluxes under a high pressure of 3–5 GPa at 1000–1100°C. Their crystal structures were determined by single-crystal X-ray diffraction techniques. All four compounds crystallize in a rhombohedral space group *R*-3*m*, *Z* = 6 with *a* = 3.6403(6) Å, *c* = 29.270(5) Å for β-ZrNBr, *a* = 3.718(2) Å, *c* = 31.381(9) Å for β-ZrNI, *a* = 3.610(1) Å, *c* = 29.294(6) Å for β-HfNBr, and *a* = 3.689(1) Å, *c* = 31.329(6) Å for β-HfNI. β-ZrNBr is isotypic with SmSI and the others are isotypic with YOF. Both structure variants are composed of structural slabs [*X*–*M*–*N*–*N*–*M*–*X*] (*M* = Zr, Hf; *X* = Br, I) stacked together by *X*...*X* van der Waals forces, but the ways of the layer stacking sequence are different: $X_AM_cN_BN_CM_bX_A|X_CM_bN_AN_BM_aX_C|X_BM_aN_CN_AM_cX_B|$ in the SmSI-type and $X_AM_bN_CN_BM_cX_A|X_CM_aN_BN_AM_bX_C|X_BM_cN_AN_CM_aX_B|$ in the YOF-type polymorphs. © 2002 Elsevier Science

INTRODUCTION

Since the discovery of the superconductivity in electron-doped β-ZrNCl and β-HfNCl with considerably high transition temperatures (T_c's) of 13 and 25.5 K for $Li_{0.16}$ZrNCl and $Li_{0.48}(THF)_y$HfNCl (THF, tetrahydrofuran), respectively (1–3), much attention has been paid to the ternary layer-structured nitrides, β-*M*N*X* (*M* = Zr, Hf; *X* = Cl, Br, I). β-ZrNCl was first prepared by Juza and Heners in 1964 (4), and Juza and Friedrichsen (5) proposed a layer-structured model, in which Cl and N atoms were close-packed and Zr atoms occupied the octahedral interstices to form a slab of [Cl–Zr–N–N–Zr–Cl], such slabs being randomly stacked in a sequence between the $CdCl_2$ (ccp) and CdI_2 (hcp) types. We developed a new synthetic route for β-ZrNCl and obtained a highly crystalline sample by the chemical transport of the as-prepared sample (6, 7). Recently, the crystal structure of β-ZrNCl was re-examined by several groups using the Rietveld analysis of powder X-ray or neutron diffraction data on the highly crystalline samples (8–11). It was revealed that β-ZrNCl was isotypic with SmSI, where the double Z–N layers in the slab were shifted so as to form new Zr–N bonds between the layers. However, the powder samples showed a very strong preferred orientation due to the layer-structured nature of the thin crystals, and thus, the structural data reported by different authors varied largely. In a previous study (12), we have succeeded in obtaining single crystals of β-ZrNCl and β-HfNCl with suitable thickness using high-pressure technique with NH_4Cl as flux, and determined the accurate crystal structures on the basis of the single crystals. All of the layer-structured nitride halides, β-*M*N*X* (*M* = Zr, Hf; *X* = Cl, Br, I) form intercalation compounds with lithium, and show superconductivity (13). As an extension of our previous study, we report here the crystal growth and the structure characterization of the remaining four members of this family, β-*M*N*X* (*M* = Zr, Hf; *X* = Br, I). Our present X-ray structure analysis has revealed that β-ZrNI, β-HfNBr, and β-HfNI are isotypic with YOF (14) rather than SmSI (15).

EXPERIMENTAL

Preparation of Single Crystals

Single crystals of β-*M*N*X* (*M* = Zr, Hf; *X* = Br, I) were prepared by the high-pressure and high-temperature technique similar to that developed in a previous study for the single crystals of β-*M*NCl (*M* = Zr, Hf) using NH_4Cl as flux (12). For the preparation of β-ZrNBr, 0.060 g (0.570 mmol) of ZrN (99%, Mitsuwa Pure Chemicals) and 0.180 g (1.838 mmol) of NH_4Br (99%, Katayama Chemical) were mixed and sealed in a platinum capsule (0.1 mm in thickness, 6 mm in inner diameter, and 4 mm in depth), which was in turn placed in a hexagonal boron nitride (h-BN) crucible, and in a cylindrical graphite tube heater. The sample assembly was set in a cube ($2.0 \times 2.0 \times 2.0$ cm^3) made

[1] To whom correspondence should be addressed. Fax: 81-824-24-7740. E-mail: syamana@hiroshima-u.ac.jp.

0022-4596/02 $35.00

of pyrophyllite and subjected to high pressure using a cubic multianvil-type apparatus (Riken, model CP-10). The reaction temperature was monitored by a thermocouple placed under the BN cell in the cube. Under an applied pressure of 3 GPa, the sample was rapidly heated at a rate of 48°C/min to 1100°C, where it was kept for 1 hour, and then cooled to 800°C at a rate of 100°C/h, followed by quenching to room temperature prior to releasing the pressure. Dark green β-ZrNBr crystals were obtained in about 30% yield. The remaining product was found to be a mixture of NH_4Br and a light yellow amorphous compound based on powder X-ray diffraction (XRD) measurements using graphite-monochromated Cu$K\alpha$ radiation. The crystals were generally grown on the surface regions of the melt contacting the wall of the Pt cell, and showed a hexagonal plate-like habit with various sizes ranging from 0.1 to 1.0 mm in diameter and several tenths of a millimeter in thickness. They were isolated by washing the reaction product with distilled water and drying with anhydrous acetone and further characterized by single-crystal X-ray diffraction measurement.

It should be mentioned that the change in temperature and the starting compositions of the reactants resulted in a significant change of the relative ratios of the phases formed. The use of the higher molar ratio (1 : 2) of ZrN/NH_4Br at a lower reaction temperature of 950°C gave an almost homogeneous β-ZrNBr powder, while the decrease of the ZrN/NH_4Br molar ratio to 1 : 5 at a higher temperature of 1200°C resulted in a lower yield of the β-ZrNBr crystals. An optimum reaction condition was reached with the ZrN/NH_4Br molar ratio of about 1 : 3, at a temperature of about 1100°C.

β-ZrNI was synthesized from a reaction using 0.050 g (0.475 mmol) of ZrN powder and 0.200 g (1.380 mmol) of NH_4I (99.5%, Katayama Chemical). The sample was introduced into a gold capsule (0.1 mm in thickness), which was again placed in a BN cell and in a carbon heater. They were heated at 1000°C for 1.5 hours under 3 GPa, then allowed to gradually cool to 850°C at a rate of 100°C/h, and finally air-quenched. Brown transparent β-ZrNI hexagonal platelets were obtained in about 40% yield. The by-product accompanying β-ZrNI was again an unknown dark yellow amorphous phase. It is noted that the thermal treatment of the same mixture of ZrN and NH_4I at 950°C under a higher pressure of 5 GPa gave similar results without generating other new phases, whereas the decrease of pressure to 1.5 GPa led to the formation of α-form of ZrNI. β-ZrNI can also be prepared by a similar high-pressure and high-temperature treatment of the corresponding α-form.

The β-HfNBr and β-HfNI crystals were grown by a two-step process. First, the powder samples of the α-forms were prepared by the reaction of NH_4Br and NH_4I, respectively, with Hf metal powder (99.9%, Mitsuwa Pure Chemicals) at 650°C, and then purified by a chemical transport reaction in the temperature gradient of 750 to 850°C as described elsewhere (6, 7). The chemically transported α-phases and the corresponding ammonium halides were filled in a molar ratio of 1 : 2.3 in Pt cells, and treated under high-pressure and high-temperature conditions as previously described at 3 GPa and 1100°C for β-HfNBr, and at 5 GPa and 1050°C for β-HfNI. The light yellow-green β-HfNBr and brown β-HfNI plate-like crystals were obtained in about 30% yield from the respective reaction products. It was important to keep the reaction temperature at 1100°C for the growth of large β-HfNBr crystals. If the temperature was lower than 950°C, no crystals larger than 0.1 mm were obtained. At temperatures higher than 1200°C, even under a high pressure of 3 GPa, β-HfNBr was decomposed to an unknown amorphous material. A summary of preparation of β-MNX (M = Zr, Hf; X = Cl, Br, I) crystals was given in Table 1.

Structure Determination

X-ray data collections of β-ZrNBr, β-ZrNI, and β-HfNBr were carried out at room temperature (298 K) on an

TABLE 1
Synthesis Conditions of β-MNX (M = Zr, Hf; X = Cl, Br, I) Single Crystals

Single crystals	Starting materials (molar ratio)	Temperature, °C	Pressure, GPa	Color	Ref.
β-ZrNCl	β-ZrNCl/NH_4Cl (1 : 3.5)	900	3	Pale yellow-green	(12)
β-ZrNBr	ZrN/NH_4Br (1 : 3.2)	1100	3	Dark green	This study
β-ZrNI	ZrN/NH_4I (1 : 2.9)	1000	3	Brown	This study
β-HfNCl	β-HfNCl/NH_4Cl (1 : 2.1)	1200	3	Colorless	(12)
β-HfNBr	α-HfNBr/NH_4Br (1 : 2.3)	1100	3	Light yellow-green	This study
β-HfNI	α-HfNI/NH_4I (1 : 2.3)	1050	5	Brown	This study

TABLE 2
Crystallographic Data for β-MNX (M = Zr, Hf; X = Br, I)

Formula	ZrNBr	ZrNI	HfNBr	HfNI
Formula weight	185.14	232.13	272.41	319.40
Crystal size, mm	$0.26 \times 0.16 \times 0.04$	$0.30 \times 0.30 \times 0.02$	$0.18 \times 0.10 \times 0.03$	$0.06 \times 0.06 \times 0.02$
Space group	$R\bar{3}m$ (No. 166)	$R\bar{3}m$ (No. 166)	$R\bar{3}m$ (No. 166)	$R\bar{3}m$ (No. 166)
a, Å	3.6403(6)	3.718(2)	3.610(1)	3.689(1)
c, Å	29.270(5)	31.381(9)	29.294(6)	31.329(6)
V, Å^3, Z	335.9(1), 6	375.7(3), 6	330.6(2), 6	369.2(2), 6
d_{calc}, g/cm^3	5.491	6.156	8.209	8.619
μ, mm^{-1}	22.309	16.322	65.005	54.519
$2\theta_{max}$, deg	100	100	100	50.6
Total reflections	1848	2108	1520	574
Unique reflection	401	454	506	116
Observed [$I \geq 2\sigma(I)$]	337	418	412	113
No. of variables	10	11	11	11
GOF[a] on F_o^2	1.147	1.171	1.103	1.274
R indices [$I \geq 2\sigma(I)$], $R1$[b]	0.0540	0.0603	0.0653	0.0544
w$R2$[c]	0.1552	0.1885	0.1464	0.1583
R indices (all data), $R1$	0.0647	0.0630	0.0851	0.0556
w$R2$	0.1602	0.1904	0.1549	0.1593

[a] $\mathrm{GOF} = \sqrt{\frac{\sum[w(F_o^2 - F_c^2)^2]}{n-p}}$, [b] $R1 = \frac{\sum\|F_o| - |F_c\|}{\sum|F_o|}$, [c] $\mathrm{w}R2 = \sqrt{\frac{\sum[w(F_o^2 - F_c^2)^2]}{\sum w(F_o^2)^2}}$.

automated Rigaku AFC7R four-circle diffractometer using monochromatized Mo$K\alpha$ radiation ($\lambda = 0.71069$ Å). Cell dimensions were obtained from a least-squares refinement with 25 automatically centered reflections in the range $32.78^\circ \leq 2\theta \leq 49.26^\circ$ for β-ZrNBr, $33.96^\circ \leq 2\theta \leq 43.89^\circ$ for β-ZrNI, and $39.79^\circ \leq 2\theta \leq 49.64^\circ$ for β-HfNBr. Three standard reflections were remeasured after every 150 reflections. No decay was observed except the statistic fluctuation in a range of $\pm$ 2.3% for β-ZrNBr, $\pm$ 0.6% for β-ZrNI, and $\pm$ 1.2% for β-HfNBr. The raw intensity data were corrected for Lorentz and polarization effects, and for absorption by empirical method based on ψ-scan data. Patterson interpretation and subsequent difference Fourier map synthesis yielded the positions of all atoms, all of which were standardized by the program STRUCTURE TIDY (16) and eventually subjected to the anisotropic refinements. An extinction correction was applied to the calculated structure factors of β-ZrNI and β-HfNBr, and refined to be 0.0002(9) and 0.0008(3), respectively. Refinement of a secondary extinction parameter in β-ZrNBr did not lead to a significant improvement in the agreement factors. Therefore, it was fixed in the final least-squares cycles. For β-ZrNBr, the final full-matrix least-squares refinements on F^2 lead to $R1 = 0.0540$ and w$R2 = 0.1552$ for 337 observed reflections ($I > 2\sigma(I)$) and 10 variables. The reliability factors for the compound β-ZrNI (β-HfNBr) converged to $R1/\mathrm{w}R2 =$ 0.0603/0.1885 (0.0653/0.1464) for 418 (412) observed reflections.

The crystal quality of β-HfNI is generally very poor. Many crystals have been examined and most of them showed broad and unsymmetric diffraction profiles in the step of searching peaks. Finally a very small one ($0.06 \times 0.06 \times 0.02$ mm^3) suitable for X-ray structure determination was found and the intensity measurements were carried out on a Rigaku RAXIS imaging plate area detector with graphite-monochromated Mo$K\alpha$ radiation operating at 50 kV and 40 mA. A total of 44 oscillation images were collected using ω scans (width of 5° and exposure time of 750 s per frame) and the empirical absorption corrections were based on the equivalent reflections. After the data reduction and averaging, the refinement of 11 parameters with 113 observed reflections resulted in the residuals of $R1/\mathrm{w}R2 =$ 0.0544/0.1583, and a secondary extinction coefficient of 0.002(1). The final difference electron density maps showed no features in all cases. Details of crystal parameters, data collection, and structure refinements are given in Table 2. All computations were performed using the SHELX97 program package (17), and crystal structure drawings were produced with ATOMS 4.0 (18). The final atomic coordinates and the equivalent isotropic and anisotropic displacement parameters are listed in Table 3, together with those of β-ZrNCl and β-HfNCl determined in a previous study (12).

RESULTS AND DISCUSSION

High-Pressure Effect

In the β-MNX (M = Zr, Hf; X = Cl, Br, I) families of compounds, the nitride chlorides can be prepared by the direct reactions of the corresponding metal or metal hydrides with ammonium chloride at elevated temperatures

TABLE 3
Atomic Coordinates and Equivalent Isotropic and Anisotropic Temperature Factors (Å^2) for β-MNX (M = Zr, Hf; X = Br, I) in Comparison with Those for β-ZrNCl and β-HfNCl

Atoms	x	y	z	$U_{11} = U_{22}$	U_{33}	$U_{23} = U_{13}$	U_{12}	U_{eq}
ZrNCl[a]								
Zr	0	0	0.11924(1)	0.0106(1)	0.0108(1)	0	0.0053(1)	0.0107(1)
Cl	0	0	0.38780(3)	0.0164(2)	0.0124(2)	0	0.0082(1)	0.0151(1)
N	0	0	0.19771(8)	0.0130(4)	0.0108(6)	0	0.0065(2)	0.0123(3)
ZrNBr								
Zr	0	0	0.12217(3)	0.0048(2)	0.0058(3)	0	0.0024(1)	0.0051(2)
Br	0	0	0.38836(3)	0.0097(3)	0.0084(3)	0	0.0048(1)	0.0093(2)
N	0	0	0.1963(2)	0.006(1)	0.006(2)	0	0.0032(6)	0.0062(9)
ZrNI								
Zr	0	0	0.20740(4)	0.0053(3)	0.0072(4)	0	0.0027(1)	0.0060(2)
I	0	0	0.38952(2)	0.0089(2)	0.0090(3)	0	0.0045(1)	0.0090(2)
N	0	0	0.1393(3)	0.005(2)	0.007(2)	0	0.0026(8)	0.006(1)
HfNCl[a]								
Hf	0	0	0.11950(1)	0.0089(1)	0.0090(1)	0	0.0044(1)	0.0089(1)
Cl	0	0	0.38795(8)	0.0127(5)	0.0111(5)	0	0.0064(2)	0.0122(3)
N	0	0	0.1976(2)	0.014(2)	0.008(2)	0	0.0067(8)	0.012(1)
HfNBr								
Hf	0	0	0.21096(3)	0.0105(2)	0.0110(3)	0	0.0053(1)	0.0107(2)
Br	0	0	0.38850(7)	0.0150(4)	0.0132(7)	0	0.0075(2)	0.0144(3)
N	0	0	0.1371(5)	0.019(4)	0.006(3)	0	0.009(2)	0.015(2)
HfNI								
Hf	0	0	0.20714(6)	0.010(1)	0.018(2)	0	0.0050(7)	0.013(1)
I	0	0	0.38960(9)	0.012(1)	0.018(2)	0	0.0060(7)	0.014(1)
N	0	0	0.1392(11)	0.011(9)	0.02(2)	0	0.005(4)	0.014(6)

Note. U_{eq} is defined as one-third of the trace of the orthogonalized **U** tensor. [a] Data taken from Ref. (12).

and ambient pressure. The as-prepared samples can be purified and changed into highly crystalline samples by the chemical transport with the aid of NH_4Cl. ZrNBr is obtained as the α-polymorph isotypic with FeOCl by a similar reaction of Zr or ZrH_2 with NH_4Br, which is changed into the β-form by the chemical transport at temperatures higher than 750°C. At a lower temperature of 450–550°C, α-ZrNBr is chemically transported as the same α-form. Since the β-form was obtained from the α-form by the thermal treatment, it had been believed that the β-form should be the high-temperature polymorph of the α-form. However, the remaining crystals, α-ZrNI, α-HfNBr, and α-HfNI, were never converted into the β-forms by a similar thermal treatment. In a previous study (19), we have pointed out that the β-forms are higher density phases and can be obtained by the transformation of the α-forms using high pressure and high temperatures. In this study, the single crystals of β-ZrNI, β-HfNBr, and β-HfNI were directly grown from NH_4Br or NH_4I fluxes under high-pressure and high-temperature conditions for the first time.

β-ZrNCl and β-HfNCl adopt the SmSI structure (12). The crystal structure of β-ZrNBr was also found to be isotypic with SmSI. In contrast, β-ZrNI, β-HfNBr, and β-HfNI, which can only be synthesized using high-pressure conditions, were found to be isostructural with YOF rather than SmSI.

Polytypes, SmSI and YOF

Both of β-MNX modifications are composed of structural slabs [X–M–N–N–M–X] (M = Zr, Hf; X = Cl, Br, I) that are stacked together by relatively weak $X \ldots X$ van der Waals forces. This is reflected by the fact that their crystals can be cleaved easily like graphite. Although the crystal structure of the SmSI-type polymorph looks very similar to those of the YOF-type (see Fig. 1), their layer stacking geometries are quite different. For the former, the anions are close-packed in $(hcch)_3$ configuration, with the X atoms in hexagonal sequence (h) and the N atoms in a cubic manner (c). The metal atoms (M) are placed in the octahedral interstices between the X and N layers, leading to the overall layer sequence of $X_AM_cN_BN_CM_bX_A|X_CM_bN_AN_BM_aX_C|X_BM_aN_CN_AM_cX_B$, while the layer sequence for the latter is $X_AM_bN_CN_BM_cX_A|X_CM_aN_BN_AM_bX_C|X_BM_cN_AN_CM_aX_B$ in which X and N atoms together form a cubic close-packed arrangement along the c-axis in the sequence ABC, or

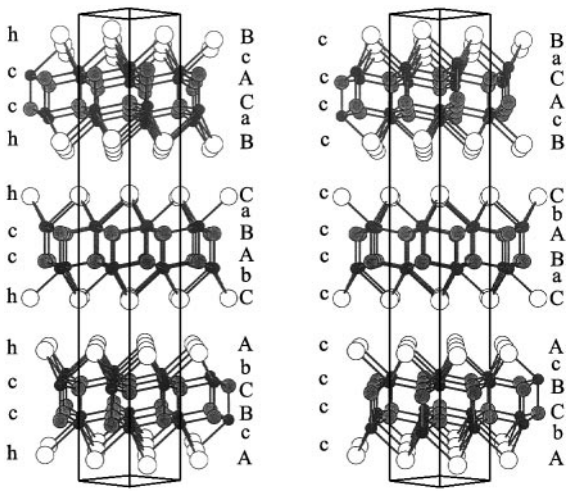

FIG. 1. View of the β-ZrNBr (SmSI-type, left) and β-HfNBr (YOF-type, right) structures along the [110] direction. Large open circles, Br; medium gray circles, N; small black circles, Zr (Hf) atoms.

$(cccc)_3$. In fact, the YOF-type phase is a stacking variant of the SmSI-type and can be derived from the latter by exchanging the sequence of the N atomic layers within the same *X*NN*X* block, accompanied by a corresponding change in the sequence of the octahedrally coordinated *M* sites.

Comparison of the Structures of β-MNX (M = Zr, Hf; X = Cl, Br, I)

Since the crystal structures of the title compounds are closely related, the discussion will refer mainly to the zirconium compounds. In β-ZrNBr, Zr and N atoms form an h-BN-like layer, which can be viewed as being sliced from the rock-salt-type nitride ZrN parallel to the (111) plane, although the hexagonal network in the latter is strongly puckered with a N–Zr–N angle of 90° (20). Two inversion-center-related Zr–N layers are condensed via the interlayer Zr–N bonds to generate a honeycomb-like bilayer that is almost planar with the N–Zr–N bond angle of 116.0(1)° (Table 4). A similar slightly distorted honeycomb lattice of the Th–N double layer has been found in thorium nitride carbide ThCN with the N–Th–N angle of 117(1)° (21). Each Zr atom is coordinated to three Br and four N atoms in a highly distorted monocapped octahedral geometry. The Zr–N bond distance for the capping N atom is about 0.025 Å larger than that for the octahedral vertex N atom (2.146(2) Å) and both are considerably shorter than the Zr–N bond distance of 2.289(1) Å in the mononitride ZrN of the rock salt type (20). The Zr–Br distances are normal, at 2.8775(8) Å, while the distance of 3.347(1) Å between adjacent Zr centers is considerably longer than that in elemental Zr (3.189 Å) (22), eliminating any significant metal–metal interactions.

In contrast to β-ZrNBr, the interlayer Zr–N distances in β-ZrNI are slightly shorter than those of the intralayer ones, but both (2.138(9)–2.187(2) Å) are still significantly smaller than that observed in ZrN. Similarly, the Hf–N distances in β-HfNBr (2.128(3)–2.165(15) Å) and β-HfNI (2.128(33)–2.168(6) Å) are also much shorter than the bond distance of 2.263(1) Å in the corresponding binary compound HfN (23). It is well known that transition metal nitrides with the rock salt structure such as ZrN and HfN show superconducting transitions at 10.7 and 8.8 K, respectively (24). On alkali-metal intercalation into β-*MNX*, electrons are doped into

TABLE 4
Selected Bond Lengths (Å) and Angles (°) for β-*MNX* (*M* = Zr, Hf; *X* = Br, I) Compared with Those in β-ZrNCl and β-HfNCl

	β-ZrNCl	β-ZrNBr	β-ZrNI	β-HfNCl	β-HfNBr	β-HfNI
Structure type	SmSI	SmSI	YOF	SmSI	YOF	YOF
Reference	(12)	This work	This work	(12)	This work	This work
M–N × 3	2.1299(5)	2.146(2)	2.187(2)	2.114(2)	2.128(3)	2.168(6)
M–N_{cap} × 1	2.172(2)	2.171(7)	2.138(9)	2.163(7)	2.165(15)	2.128(33)
M–*X* × 3	2.7465(6)	2.8775(8)	3.066(1)	2.738(2)	2.867(2)	3.055(2)
M–*M*** × 3	3.3498(5)	3.347(1)	3.338(2)	3.3313(7)	3.328(1)	3.312(3)
X … *X** × 6	3.6046(4)	3.6403(6)	3.718(2)	3.5767(8)	3.610(1)	3.689(1)
X … *X*** × 3	3.663(1)	3.846(2)	4.129(2)	3.664(4)	3.846(4)	4.119(5)
N–*M*–*N* × 3	115.60(4)	116.0(1)	116.4(2)	115.6(1)	116.0(3)	116.6(5)
N–M–N_{cap} × 3	77.71(6)	78.3(2)	79.0(2)	77.7(2)	78.3(4)	79.2(9)
N–*M*–*X* × 3	151.55(6)	148.6(2)	145.5(2)	151.3(2)	148.3(4)	145.0(9)
N–*M*–*X* × 3	76.63(5)	77.3(1)	78.1(2)	76.8(1)	77.5(3)	78.0(7)
N_{cap}–*M*–*X* × 3	130.74(1)	133.08(2)	135.55(3)	131.05(4)	133.37(4)	135.81(4)
X–*M*–*X* × 3	82.02(2)	78.48(3)	74.66(4)	81.55(6)	78.04(5)	74.27(7)

Note. * and ** represent intralayer and interlayer distances, respectively.

the MN double layers, giving the metallic behavior and superconductivity as well. Some reasons for the remarkably high T_c's observed for the electron-doped β-MNX could be found in the shorter M–N bond distances, and in the coplanarity of the double M–N layers, compared with those of the corresponding binary nitrides.

β-MNX is characterized by the rigid two-dimensional M–N networks accommodating the compressed halogen ions. This is reflected by the fact that the intralayer X–X distances only slightly increase, while the interlayer $X \ldots X$ distances significantly increase with the halogen radius (Table 4). It also explains why a high pressure of at least 5 GPa is required to compress the large iodine ions into the small Hf–N framework to form the β-HfNI phase (Table 1). A comparison of the β-ZrNCl, β-ZrNBr, and β-ZrNI structures reveals that the double Zr–N layers become slightly flatter with the increase of the halogen radius irrespective of the stacking variant being present in the crystal structure of the particular compound, as seen from the N–Zr–N angles in Table 4. The in-plane Zr–N distances are monotonically increased on going from ZrNCl (2.1299(5) Å), ZrNBr (2.146(2) Å), to ZrNI (2.187(2) Å). The Zr–N interlayer distances in the double layers undergo almost no change upon substitution of the larger bromine for chlorine. In the three compounds mentioned above, zirconium atoms are displaced out of the center of the octahedron toward the capped N_3 face by 0.461 Å in β-ZrNCl, 0.549 Å in β-ZrNBr, and 0.682 Å in β-ZrNI, which is responsible for the angle changes in Table 4. It is believed that this shift is at least partially driven by the size difference between the nitrogen and halide ions. A similar situation has also been observed in the series of the Hf compounds, except that the bond distances around the Hf atom in β-HfNX are all smaller than the corresponding distances for the Zr atom in the zirconium analogue. An examination of the effects of substitution of halogens and metals in β-MNX (M = Zr, Hf; X = Cl, Br, I) on the superconductivity of the electron-doped compounds (13) indicated that the T_c's of the lithium-intercalated phases were predominantly determined by the kinds of nitride layers (ZrN or HfN) and the short in-plane M–N distances are generally favorable for the high T_c. The substitution of halogen atoms hardly influenced the superconducting properties. It is also interesting to note that the changes of the structure type of the β-MNX host lattices (SmSI or YOF) do not influence the T_c values of the lithium-intercalated phases. These results further confirm that the origin of superconductivity is to be sought in the central M–N–N–M part of the slab.

Related Layer Structures

β-MNX (M = Zr, Hf; X = Cl, Br, I) can also be described as a filled-up version of the ZrCl or ZrBr stacking polytype structure. It is well known that many of the early transition metals form unusual monohalides MX (M = Zr, Hf; X = Cl, Br) in which the cubic close-packed layers of metal and halide atoms are stacked in pairs to yield the sequence X–M–M–X with relative orientations AbcA. These tightly bound four-layer slabs occur in two stacking sequences, either $X_A M_b M_c X_A | X_B M_c M_a X_B | X_C M_a M_b X_C$ (briefly ABC, designating outer halogen layers only) in the ZrCl type (25) or $X_A M_b M_c X_A | X_C M_a M_b X_C | X_B M_c M_a X_B$ (ACB) in the ZrBr form (26), both having characteristic van der Waals gaps between halogen layers of adjacent slabs. The same structures have been reported for ScCl, YCl, and many of the lanthanide chlorides and bromides LnX (X = Cl, Br), although it was subsequently found that all the monohalides of the trivalent elements are actually ternary phases $LnXH_x$ stabilized by hydrogen (27, 28). The insertion of the nitrogen atoms in all of the tetrahedral holes between the double metal layers of ZrCl and ZrBr will give the β-ZrNCl (SmSI-type) and β-ZrNI (YOF-type) structures, respectively, whereas the filling of the octahedral interstitial voids of $LnXH_x$ with C_2 pairs will result in the superconducting carbide halides $Ln_2C_2X_2$ (Ln = La, Y, Lu; X = Br, I) which also crystallize in two polymorphs: the 1 s form with a periodicity AβcαB (based on the parent ZrCl structure), and the 3 s form with a periodicity AβcαB|CαbγA|BγaβC (derived from the ZrBr structure) (X = A, B, C; C$_2$ = a, b, c; Ln = α, β, γ) (29). In fact, β-ZrNCl, ZrCl, β-ZrNI, and ZrBr crystallize in the same space group with similar unit cells. The space group $C2/m$ of $Ln_2C_2X_2$ is a "*translationengleiche*" subgroup (index 3) of the group R-3m adopted by β-MNX. The lattice vectors of $Ln_2C_2X_2$ (**a**, **b**, and **c**) are related to those of β-MNX ($\mathbf{a_1}$, $\mathbf{a_2}$, and $\mathbf{a_3}$) in the following manner: $\mathbf{a} = \mathbf{a_1} + 2\mathbf{a_2}$, $\mathbf{b} = \mathbf{a_1}$, and $\mathbf{c} = -1/3\mathbf{a_1} - 2/3\mathbf{a_2} - 1/3\mathbf{a_3}$.

CONCLUSIONS

In the literature, two groups reported their Rietveld refinements of the β-ZrNBr structure based on powder X-ray diffraction data (8, 9). However, the powder sample showed a very strong preferred orientation due to the layer-structured characteristic of the crystals, and the geometrical parameters of β-ZrNBr determined by these authors are not precise and deviate slightly from our results. For example, for the interlayer Zr–N_{cap} distance, Fuertes *et al.* (8) gave 2.30(4) Å, while Fogg *et al.* (9) reported a larger value of 2.44(2) Å. Our present single-crystal analysis data are more accurate owing to the larger reflection number/parameter number ratio used (> 30) and produced a shorter Zr–N_{cap} bond length of 2.171(7) Å, with about 3 times smaller standard deviations. The crystal structures of three high-pressure phases, β-ZrNI, β-HfNBr, and β-HfNI, were presented here for the first time, a preliminary account of the existence of which has been given by us earlier (19).

ACKNOWLEDGMENTS

This study has been supported by Grant-in-Aid for Scientific Research (B) (No. 12450353) and the COE Research (No. 13CE2002) of the Ministry of Education, Culture, Sports, Science and Technology of Japan.

REFERENCES

1. S. Yamanaka, H. Kawaji, K. Hotehama, and M. Ohashi, *Adv. Mater.* **8,** 771–774 (1996).
2. S. Yamanaka, K. Hotehama, and H. Kawaji, *Nature* **392,** 580–582 (1998).
3. S. Yamanaka, *Annu. Rev. Mater. Sci.* **30,** 53–82 (2000).
4. R. Juza and J. Heners, *Z. Anorg. Allg. Chem.* **332,** 159–172 (1964).
5. R. Juza and H. Friedrichsen, *Z. Anorg. Allg. Chem.* **332,** 173–178 (1964).
6. M. Ohashi, S. Yamanaka, M. Sumihara, and M. Hattori, *J. Solid State Chem.* **75,** 99–104 (1988).
7. M. Ohashi, S. Yamanaka, and M. Hattori, *J. Solid State Chem.* **77,** 342–347 (1988).
8. (a) A. Fuertes, M. Vlassov, D. Beltrán-Porter, P. Alemany, E. Canadell, N. Casañ-Pastor, and M. R. Palacín, *Chem. Mater.* **11,** 203–206 (1999); (b) M. Vlassov, M. R. Palacín, D. Beltrán-Porter, J. Oró-Solé, E. Canadell, P. Alemany, and A. Fuertes, *Inorg. Chem.* **38,** 4530–4538 (1999).
9. (a) A. M. Fogg, J. S. O. Evans, and D. O'Hare, *Chem. Commun.* **20,** 2269–2270 (1998); (b) A. M. Fogg, V. M. Green, and D. O'Hare, *J. Mater. Chem.* **9,** 1547–1551 (1999).
10. S. Y. Istomin, J. Köhler, and A. Simon, *Physica C* **319,** 219–228 (1999).
11. S. Shamoto, T. Kato, Y. Ono, Y. Miyazaki, K. Ohoyama, M. Ohashi, Y. Yamaguchi, and T. Kajitani, *Physica C* **306,** 7–14 (1998).
12. X. Chen, T. Koiwasaki, and S. Yamanaka, *J. Solid State Chem.* **159,** 80–86 (2001).
13. S. Yamanaka, K. Hotehama, T. Koiwasaki, H. Kawaji, H. Fukuoka, S. Shamoto, and T. Kajitani, *Physica C* **341–348,** 699–702 (2000).
14. A. W. Mann and D. J. M. Bevan, *Acta Crystallogr. B* **26,** 2129–2131 (1970).
15. H. P. Beck and C. Strobel, *Z. Anorg. Allg. Chem.* **535,** 229–239 (1986).
16. L. M. Gelato and E. Parthé, *J. Appl. Crystallogr.* **20,** 139–143 (1987).
17. G. M. Sheldrick, SHELX-97: program for structure refinement; University of Goettingen, Germany, 1997.
18. ATOMS V4.0 for Windows, Shape Software, 2000.
19. S. Yamanaka, K. Itoh, H. Fukuoka, and M. Yasukawa, *Inorg. Chem.* **39,** 806–809 (2000).
20. JCPDS card 35-753.
21. R. Benz, G. P. Arnold, and W. H. Zachariasen, *Acta Crystallogr. B* **28,** 1724–1727 (1972).
22. J. Haglund, F. Fernandez Guillermet, G. Grimvall, and M. Korling, *Phys. Rev. B* **48,** 11685–11691 (1993).
23. JCPDS card 33-592.
24. B. W. Roberts, *J. Phys. Chem. Ref. Data* **5,** 581–795 (1976).
25. D. G. Adolphson and J. D. Corbett, *Inorg. Chem.* **15,** 1820–1823 (1976).
26. R. L. Daake and J. D. Corbett, *Inorg. Chem.* **16,** 2029–2033 (1977).
27. A. Simon, *J. Solid State Chem.* **57,** 2–16 (1985).
28. G. Meyer, S.-J. Hwu, S. Wijeyesekera, and J. D. Corbett, *Inorg. Chem.* **25,** 4811–4818 (1986).
29. A. Simon, A. Yoshiasa, M. Bäcker, R. W. Henn, C. Felser, R. K. Kremer, and Hj. Mattausch, *Z. Anorg. Allg. Chem.* **622,** 123–137 (1996).